Evanescent wave ammonia sensor: influence of nanocrystalline TiO_2 on V_2O_5 and MoO_3

Paramasivam Chandrasekar[1], *Thangaraj Subashini*[2], *Balusamy Renganathan*[3], *Thanigainathan Prakash*[2] ✉

[1]*Geetha Jeevan Arts and Science College, Kurukkusalai, Thoothukudi 628722, India*
[2]*National Centre for Nanoscience and Nanotechnology, University of Madras, Guindy Campus, Chennai 600025, India*
[3]*Applied Optics Laboratory, Indian Institute of Technology Madras, Chennai 600036, India*
✉ *E-mail: thanigaiprakash@gmail.com*

Published in Micro & Nano Letters; Received on 19th July 2019; Revised on 8th September 2019; Accepted on 18th September 2019

Clad-modified fibre optic ammonia sensor was developed subsequently using pure V_2O_5, MoO_3, and its composites with TiO_2. Prior to the sensing measurement, the composite was synthesised and studied for the structural and microstructural properties using powder X-ray diffractometer and field emission scanning electron microscope. The analysis confirms the existence of nanocrystalline anatase phase TiO_2 in the grain boundaries of microcrystalline V_2O_5/MoO_3 in the composites. Ammonia sensing measurement was performed for different concentrations of ammonia exposures up to 500 ppm. The obtained response was applied to calculate the sensitivity and it was found to be superior for the clad modified with composite material as compared to the pure microcrystalline samples are discussed in detail.

1. Introduction: Materials with modified properties are being developed to fabricate the high definition sensor that exhibits superior sensitivity and selectivity. Recent technological advancements in sensor manufacture and the materials development have gained considerable attention in the scientific world [1]. Fibre optic sensors are being made with interest and increasing effect due to their inherent advantages such as simplicity of operation, low cost, multiplexing proficiency, and ability to perform as real dispersed sensors [2]. In fibre optic sensors, the intensity modulation can be altered with interchange or modified with the small portion of the cladding part of the optical fibre, called clad-modified optical fibre sensors [3]. In general, the mechanism of clad-modified fibre optic sensor is based on the evanescent wave absorption technique. In fibre optic gas sensors, the evanescent wave changed with changes in the refractive index of the sensing material when exposed to the desired gas [4]. Up to now, various kinds of gas sensors, including metal oxide gas sensor, polymer composite gas sensor, carbon nanotube-based gas sensor, and nanoheterostructural gas sensor have been extensively investigated [5–7]. There are several transition metal oxides such as ZnO, SnO_2–CuO, NiO, V_2O_5, and WO_3 [8–11], which have been used for fibre optic gas sensor applications by various researchers. Nevertheless, such bulk material is hampered to achieve superior sensitivity and response which prompts to discover the micro–nano-composite to improve the performance. The reason for finding such innovations is a high surface area, size effect, and enhanced reaction mechanism on the surface of micro–nano-composite among others. Micro–nano-composite consists of a large number of grains contacting at microcrystalline boundaries.

Ammonia sensor has been used for medical diagnostic breath analysis, automotive air quality monitoring, warfare, and explosive agents monitoring, environmental monitoring, refrigeration, agricultural monitoring and chemical industry monitoring [12]. The long-term exposure above 500 ppm concentration can create an accumulation of fluid in the lungs causing pulmonary oedema [13]. The low concentration of ammonia does not cause severe problems to humans since it is a natural body product from the metabolic reaction of protein and nucleic acid. The resulting metabolic product from the body, such as urea and ammonium salts, excreted through sweating glands. Although excess ammonia in exhaled air is symptoms of kidney disorder or ulcers caused by *Helicobacter pylori* bacteria which is on the wall of the human stomach and neutralising the digestive acid to survive. Gaston *et al.* [14] reported that the sensors based on the parameters of temperature, humidity, and pH using clad-modified technique may lead to performing high sensitivity, low attenuation, and high propagation strength.

Studies on the surface modification of TiO_2 with vanadium species improve the ethanol gas sensitivity up to two orders over pure TiO_2 was recently reported by Epifani *et al.* [15]. Galatsis *et al.* [16] investigated O_2, CO and NO_2 gas sensing properties of the sol–gel-derived MoO_3–TiO_2 thin films. Comparative study of gas sensing behaviour of MoO_3 thin films prepared by the different synthesis methods was demonstrated by Prasad *et al.* [17]. The reason for selecting the specific transition metal oxides V_2O_5 and MoO_3 is similar in the crystal structure, ionic radii, and their highest oxidation state providing the unique intercalation of gas molecules [18]. In this paper, micro–nano-composites were prepared and it is coated as a modified clad material in the small region of optical fibre to fabricate the ammonia sensor. The structural and ammonia gas sensing properties of the microcrystalline V_2O_5 and MoO_3 samples and their composite with TiO_2 were studied. The sensing performance of the composites was studied in ammonia gas at room temperature using the evanescent wave adsorption.

2. Experimental details: Anatase phase titanium dioxide nanocrystals were prepared by the sol–gel method using titanium (IV) tetraisopropoxide ($C_{12}H_{28}O_4Ti$, Sigma-Aldrich) as a precursor. The detailed synthesis condition was reported elsewhere [19]. Vanadium pentoxide (V_2O_5, SRL) and molybdenum trioxide (MoO_3, Alfa aesar) were directly used without any further purification. The micro–nano-composites were prepared by mixing 0.95:0.05 weight ratio, the resulting powder was ground to obtain a fine mixture using pestle and mortar, then the samples were annealed at 450°C for 1 h under high-temperature box furnace. Powder X-ray diffraction patterns recorded on the Rigaku Ultima-IV powder X-ray diffractometer using $CuK_{\alpha 1}$ radiation ($\lambda = 0.15406$ nm). The sol–gel-derived nanocrystalline TiO_2 sample was collected by Philips CM12 transmission electron microscope to understand the crystallite size distribution and its morphology. Morphology of all the four samples was carried out using a Zeiss SUPRA 40 FESEM microscope operated at 20 kV.

doi: 10.1049/mnl.2019.0451

The clad-modified fibre optic sensor was prepared using polymethylmethacrylate (PMMA) fibre with a clad diameter and refractive index of 15 μm and 1.402, respectively. The refractive index of the core is about 1.492. However, in this case, we are concerned about the refractive index of the clad. The sensitivity of the sensor increased with an increase in the refractive index of the coated fibre reported in the earlier literature [20]. The total length of the fibre used for this Letter is about 42 cm and the middle portion of the clad was removed using the mechanical scrubbing process. Further, the unclad portion of the optical fibre was coated with the samples by a slurry deposition method using isopropanol as a solvent. Ammonia sensing characteristics of the samples were studied using indigenously designed gas-sensor set-up [11]. The variations in the optical intensity of the pure and composite samples were obtained using the computer controlled spectrophotometer (EPP-2000, Stellar Net Inc., USA) in the range of 190–1100 nm.

3. Results and discussion

3.1. Structural analysis: Structural properties of sol–gel-derived nanocrystalline TiO_2, microcrystalline, and micro–nano-composites were analysed using powder X-ray diffraction and shown, respectively, in Figs. 1*a*–*e*. All the peaks present in Fig. 1*a* were well indexed with the joint committee for powder diffraction standard JCPDS Card No. 89–4921 using the XRDA 3.1 software and the peaks were assigned to the anatase TiO_2 phase with the planes of (101), (004), (200), (105), and (211). In the micro–nano-composite, only peaks corresponding to the orthorhombic V_2O_5 and MoO_3 were found in the XRD pattern according to the JCPDS Card Nos. 09-0387 and 05-0508, respectively.

3.2. Microstructural analysis: The nanocrystalline nature of the TiO_2 sample was confirmed directly with bright field transmission electron microscopic image shown in Fig. 2*a*. The average grain size was calculated and shown in the image of Fig. 2*b*. The best fit of this distribution was achieved with a Gaussian function, shown as a red solid line and the average grain size is about 9 nm. Selected area electron diffraction pattern of the sol–gel-derived TiO_2 was converted into three dimensions using the commercial Image-J scientific software and it was shown as Fig. 2*c*. The obtained electron diffraction pattern was indexed [21] with the anatase phase of TiO_2 and the rings are assigned to (101), (004), (200), and (105).

The microstructural analysis of pure V_2O_5, MoO_3, and micro–nano-composites was shown in Figs. 3*a*–*d*, respectively. It can be seen that the samples depicted in Figs. 3*b* and *d* composed of micro- and nanoscale materials clearly reveal the formation of the

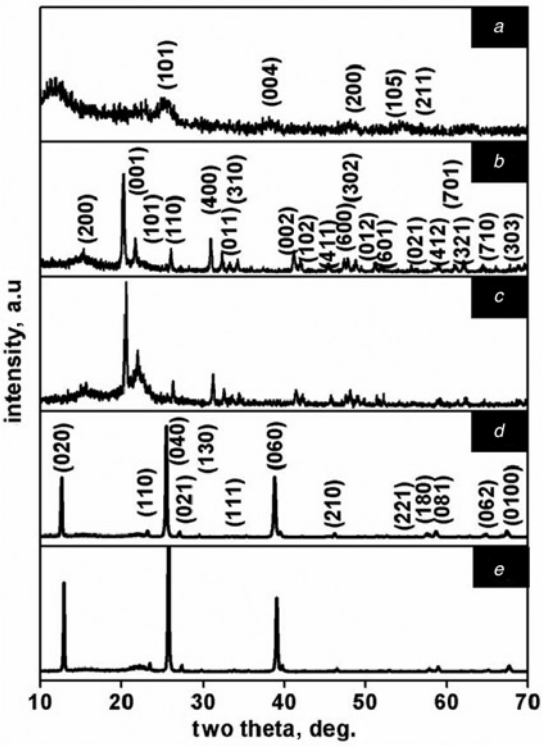

Fig. 1 *Powder X-ray diffraction pattern of*
a Nanocrystalline TiO_2
b Microcrystalline V_2O_5
c $(V_2O_5)_{0.95}$–$(TiO_2)_{0.05}$ composite
d Microcrystalline MoO_3
e $(MoO_3)_{0.95}$–$(TiO_2)_{0.05}$ composite

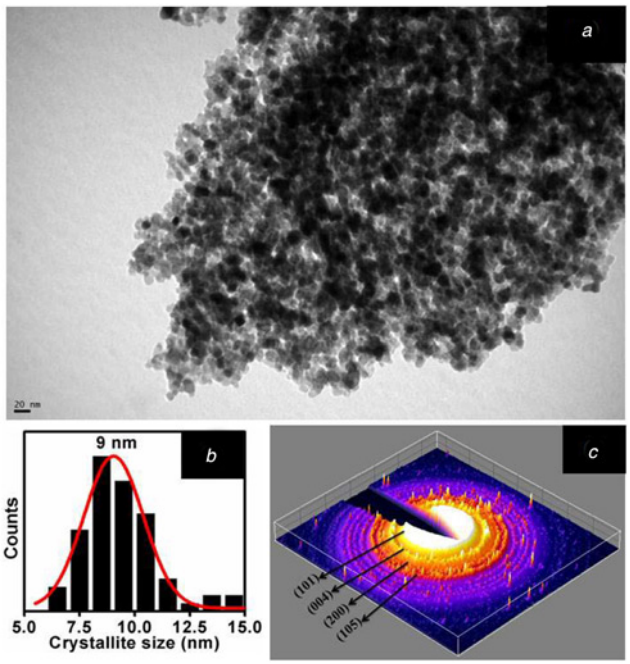

Fig. 2 *Nanocrystalline TiO_2*
a HRTEM image
b Crystallite size distribution
c Selected area electron diffraction pattern

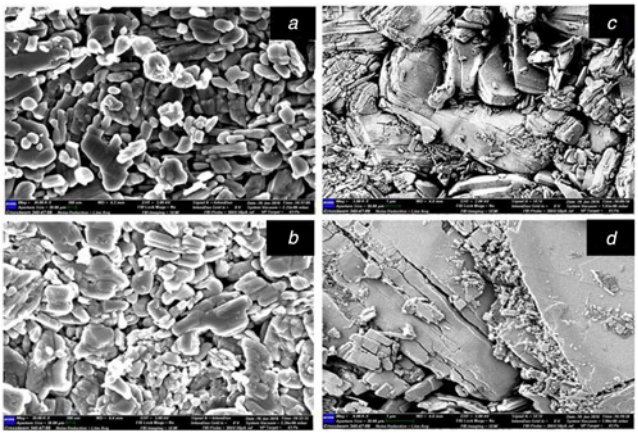

Fig. 3 *FESEM images of*
a Microcrystalline V_2O_5
b $(V_2O_5)_{0.95}$–$(TiO_2)_{0.05}$ composite
c Microcrystalline MoO_3
d $(MoO_3)_{0.95}$–$(TiO_2)_{0.05}$ composite

micro–nano-composite. The V_2O_5 and MoO_3 exhibit irregular microdimension flakes like morphology and the TiO_2 crystallites were distributed on the grain boundaries of microcrystalline materials. The microstructural analysis reveals the dimension of crystallites in the micro- and nanoregime of the composite sample.

3.3. Fibre optic ammonia sensing behaviour: A clad-modified fibre optic sensor was made by mechanical scrubbing of the clad part of the fibre to expose the core surface over a length of 3 cm. All the four samples were formed into a paste by adding a few drops of 2-propanol then the paste was coated on the fibre optic cable where the clad is removed and then dried under air. The coating thickness on the clad removal part is about 30 µm [10]. The principle of an optical fibre is total internal reflection [22] when it applied to the interface of the core-modified clad, all the intensity has not reflected back at the interface and some part of intensity has penetrated into the modified clad part and that intensity is called evanescent wave which decays exponentially away from the interface. In this clad-modified fibre one end of the fibre is connected to the source while the other end of the fibre is connected to the detector. The light waves propagate through one end of the fibre while the other end the optical signal attenuation will be detected by a detector. This optical attenuation was due to the evanescent field produced by the coated material in the clad-modified region of the optical fibre.

The block diagram of the clad-modified optical fibre ammonia gas sensing set-up along with the mechanism of light transmission in clad-modified fibre was shown in Fig. 4. Here the samples composed of both the micro- and nanoregime materials and nanocrystalline TiO_2 consist of a large number of grains, contacting at V_2O_5 and MoO_3 boundaries. Due to this reason, the large numbers of ammonia molecules were accumulated in the active sites of sensing materials [23]. The ammonia sensing behaviour of pure and micro–nano-composite samples at concentrations from 0 to 500 ppm in the periodic interval of 10 min was investigated using a fibre optic spectrophotometer. The obtained spectral response was shown in Figs. 5*a*–*d* and its magnified spectral response was shown as an inset. From this spectral response, the intensity of the dip wavelength increases with the increasing of ammonia gas concentration due to the reducing nature of ammonia molecules. The observed dip wavelengths in the spectral responses are 711 and 758 nm for all the samples. From the analysis of sensitivity data, it is inferred that only micro–nano-composite showed superior spectral response at 758 nm when compared to pure samples. The gas sensitivity of the clad-modified optical fibre gas sensor is associated with spectral intensity of samples and it can be calculated using the equation $S\ (\%) = ((I_o - I_g)/I_o) \times 100$, where I_o is the spectral intensity in the absence of gas and I_g is the spectral intensity in the presence of gas. It was observed that the micro–nano-composites of V_2O_5 and MoO_3 samples showed the sensitivity of 3.9 and 4.9% when compared with the sensitivity of pure microcrystalline V_2O_5 and MoO_3 about 2.1

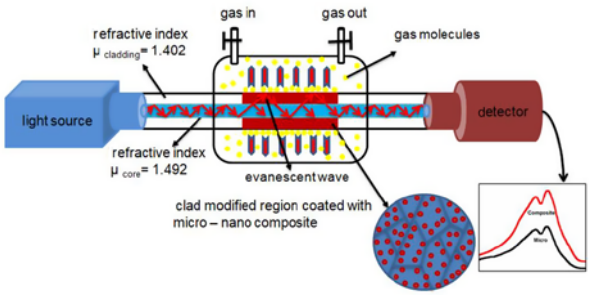

Fig. 4 *Block diagram of an evanescent wave ammonia gas sensor measurement set-up*

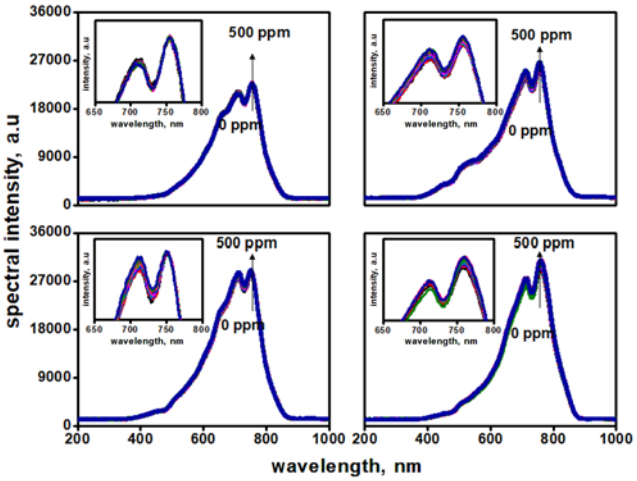

Fig. 5 *Spectral response of optical fibre clad modified with*
a Microcrystalline V_2O_5
b $(V_2O_5)_{0.95}$–$(TiO_2)_{0.05}$ composite
c Microcrystalline MoO_3
d $(MoO_3)_{0.95}$–$(TiO_2)_{0.05}$ composite for different concentration of ammonia
(Inset: Magnified spectral response)

and 3.7%, respectively, at 500 ppm of ammonia gas concentration. In order to identify the superior sensitivity and nature of the composites, all the data were plotted in the bar chart representation as shown in Figs. 6*a* and *b*. We have found that the sensitivity of samples linearly increases with an increase in ammonia concentration. Further, the micro–nano-composites exhibited superior sensitivity towards the ammonia gas compared to the microcrystalline samples due to the grain boundary effects in polycrystalline inorganic TiO_2 working at room temperature. The improved sensitivity was due to the presence of nanocrystalline titania grains, segregated at the microcrystalline sample grain boundary enhances the surface area of the composite material. Hence, the impact on the surface area leads to accumulating more reducing ammonia molecules which donate their valence electrons to the sample which modifies the refractive index of the sensing material [24]. The unique layered structure of both V_2O_5 and MoO_3 along with the enhanced surface area due to the nanocrystalline leads to the intercalation of ammonia molecules into their active sites showing the superior sensitivity.

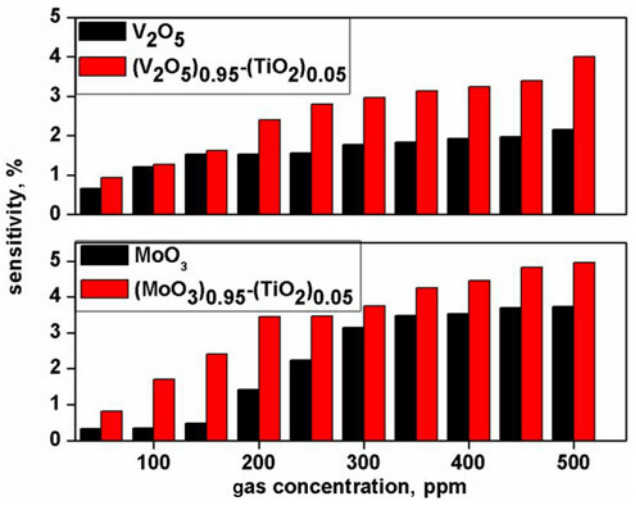

Fig. 6 *Concentration-dependent percentage sensitivity plot for pure V_2O_5, MoO_3 micro-V_2O_5–nano-TiO_2 and micro-MoO_3–nano-TiO_2 composites*

doi: 10.1049/mnl.2019.0451

4. Conclusion: A clad-modified fibre optic ammonia sensor was developed subsequently using pure V_2O_5, MoO_3, and its composites with TiO_2. The sensing measurement was performed for different concentrations of ammonia exposures up to 500 ppm. The sensitivity of the V_2O_5 and MoO_3 samples was 3.9 and 4.9%, respectively, showed a superior sensitivity when compared to the pure microcrystalline samples. As expected, the micro–nano-composite showed a higher sensitivity than the microcrystalline samples, which are due to the enhanced surface area of the composite samples in the presence of nanocrystalline titania, led to accumulating more gaseous ammonia molecules. Therefore, the evaluations of prepared micro–nano-composite samples are suitable for the ammonia sensor.

5. Acknowledgments: This research work was supported by the Science and Engineering Research Board (SERB), India under the sponsored major research project number YSS/2014/000243 dated 31 December 2015.

6 References

[1] Dai Z., Liang T., Lee J.H.: 'Gas sensors using ordered macroporous oxide nanostructures', *Nanoscale Adv.*, 2019, **1**, pp. 1626–1639
[2] Pathak A., Mishra S.K., Gupta B.D.: 'Fiber-optic ammonia sensor using Ag/SnO_2 thin films: optimization of thickness of SnO_2 film using electric field distribution and reaction factor', *Appl. Opt.*, 2015, **54**, (29), pp. 8712–8721
[3] Arie A., Karoubi R., Gur Y.S., *ET AL.*: 'Measurement and analysis of light transmission through a modified cladding optical fiber with applications to sensors', *Appl. Opt.*, 1986, **25**, (11), pp. 1754–1758
[4] Nazemi H., Joseph A., Park J., *ET AL.*: 'Advanced micro- and nano-gas sensor technology: a review', *Sensors*, 2019, **19**, (6), p. 1285
[5] Wang C., Yin L., Zhang L., *ET AL.*: 'Metal oxide gas sensors: sensitivity and influencing factors', *Sensors*, 2010, **10**, (3), pp. 2088–2106
[6] Adhikari B., Majumdar S.: 'Polymers in sensor applications', *Prog. Polym. Sci.*, 2004, **29**, (7), pp. 699–766
[7] Zaporotskova I.V., Boroznina N.P., Parkhomenko Y.N., *ET AL.*: 'Carbon nanotubes: sensor properties. A review', *Mod. Electron. Mater.*, 2016, **2**, (4), pp. 95–105
[8] Zhu Y., Fu H., Ding J., *ET AL.*: 'Fabrication of three-dimensional zinc oxide nanoflowers for high- sensitivity fiber-optic ammonia gas sensors', *Appl. Opt.*, 2018, **57**, (27), pp. 7924–7930
[9] Mariammal R.N., Ramachandran K., Renganathan B., *ET AL.*: 'On the enhancement of ethanol sensing by CuO modified SnO_2 nanoparticles using fiber optic sensor', *Sensor Actuat. B: Chem.*, 2012, **169**, pp. 199–207
[10] Yamini K., Renganathan B., Ganesan A.R., *ET AL.*: 'Clad modified optical fiber gas sensors based on nanocrystalline nickel oxide embedded coatings', *Opt. Fiber Technol.*, 2017, **36**, pp. 139–143
[11] Renganathanan B., Sastikumar D., Gokul Raj S., *ET AL.*: 'Fiber optic gas sensors with vanadium oxide and tungsten oxide nanoparticle coated claddings', *Opt. Commun.*, 2014, **315**, pp. 74–78
[12] Khan H., Malook K., Shah M.: 'Highly selective and sensitive ammonia sensor using polypyrrole/V_2O_5 composites', *J. Mater. Sci.: Mater. Electron.*, 2017, **28**, (18), pp. 13873–13879
[13] Timmer B., Olthuis W., Berg A.: 'Ammonia sensors and their applications – a review', *Sensor Actuat. B: Chem.*, 2005, **107**, (2), pp. 666–677
[14] Gaston A., Lozano I., Perez F., *ET AL.*: 'Evanescent wave optical-fiber sensing (temperature, relative humidity, and pH sensors)', *IEEE Sens. J.*, 2003, **3**, (6), pp. 806–811
[15] Epifani M., Díaz R., Force C., *ET AL.*: 'Colloidal counterpart of the TiO_2 supported V_2O_5 system: a case study of oxide-on-oxide deposition by wet chemical techniques. Synthesis, vanadium speciation, and gas sensing enhancement', *J. Phys. Chem. C*, 2013, **117**, (40), pp. 20697–20705
[16] Galatsis K., Li Y.X., Wlodarski W., *ET AL.*: 'Semiconductor MoO_3–TiO_2 thin film gas sensors', *Sensor Actuat. B: Chem.*, 2001, **77**, (1–2), pp. 472–477
[17] Prasad A.K., Kubinski D.J., Gouma P.I.: 'Comparison of sol-gel and ion beam deposited MoO_3 thin film gas sensors for selective ammonia detection', *Sensor Actuat. B: Chem.*, 2003, **93**, (1–3), pp. 25–30
[18] Imavan C., Steffs H., Solzbacher F., *ET AL.*: 'Structural and gas sensing properties of V_2O_5-MoO_3 thin films for H_2 detection', *Sensor Actuat. B: Chem.*, 2001, **77**, (1–2), pp. 346–351
[19] Prakash T., Ramasamy S., Murty B.S.: 'Influence of bias voltage on dielectric relaxation of nanocrystalline anatase TiO_2 using modulus formalism', *J. Appl. Phys.*, 2011, **109**, (8), p. 084116
[20] Li X., Li S., Yan X., *ET AL.*: 'High sensitivity photonic crystal fiber refractive index sensor with gold coated externally based on surface plasmon resonance', *Micromachines (Basel)*, 2018, **9**, (12), p. 640
[21] Shaikh S.F., Ghule B.G., Nakate U.T., *ET AL.*: 'Low-temperature ionic layer adsorption and reaction grown anatase TiO_2 nanocrystalline films for efficient perovskite solar cell and gas sensor applications', *Sci. Rep.*, 2018, **8**, (1), p. 11016
[22] Devendiran S., Sastikumar D.: 'Gas sensing based on detection of light radiation from a region of modified cladding (nanocrystalline ZnO) of an optical fiber', *Opt. Laser Technol.*, 2017, **89**, pp. 186–191
[23] Wang L., Chen S., Li W., *ET AL.*: 'Grain-boundary-induced drastic sensing performance enhancement of polycrystalline-microwire printed gas sensors', *Adv. Mater.*, 2019, **31**, (4), p. 1804583
[24] Pawar D., Kale S.N.: 'A review on nanomaterials-modified optical fiber sensors for gases, vapors and ions', *Microchim. Acta*, 2019, **186**, (4), p. 253